



## Highest Pressure Adsorption Equilibria Data: Measurement with Magnetic Suspension Balance and Analysis with a New Adsorbent/Adsorbate-Volume

F. DREISBACH AND H.W. LÖSCH

*Rubotherm Präzisionsmeßtechnik GmbH, Universitätsstr. 142, 44799 Bochum, Germany*

P. HARTING

*Institut für Nichtklassische Chemie an der Universität Leipzig, Permoserstr. 15, 04318 Leipzig, Germany*

*Received September 6, 2001; Revised January 31, 2002; Accepted February 11, 2002*

**Abstract.** Adsorption data at high pressures provide information about properties of the adsorbent material and about the structure of the adsorbed phase. In order to obtain this information adsorption processes need to be measured in a wide pressure range and require careful experimental data handling. In this paper, an experimental installation with a magnetic suspension balance for the gravimetric measurement of adsorption equilibria data at pressures still inaccessible for this experimental technique will be presented. Using this instrument the adsorption data of He, CH<sub>4</sub>, N<sub>2</sub> and Ar on a microporous activated carbon are measured at pressures up to 50 MPa at  $T = 298.15$  K. The resulting data allow a critical discussion of the commonly used model for the volume of the adsorbent material (i.e. the Helium-volume). As a result of this, a new model for the volume of the adsorbed phase is proposed. This volume model allows to calculate a pressure dependent density of the adsorbed phase. The model and the resulting densities of the adsorbed phase are discussed concerning their physical sensitivity.

**Keywords:** gas adsorption equilibria, high pressure, buoyancy correction, density of adsorbed phase, compressibility of adsorbed phase

### Introduction

Adsorption equilibria data in both high and highest pressure ranges are important from a scientific point of view. However, too little is known about the behavior of adsorbent material under high pressures. This is of technical importance when considering pressures exerted on adsorbents in Mercury intrusion experiments for the determination of adsorbent characteristics and any changes to the adsorbent materials which may be caused. Moreover, the behavior of the adsorbed phase under high adsorptive pressures also still has to be examined, in particular the behavior of the so-called excess quantities at high pressures and their analytical representation by adsorption models. In addition, the density of an adsorbate on the pores and the surface of an adsorbent is an unknown property. In order to

address these issues the adsorption of technically important gases such as He, CH<sub>4</sub>, N<sub>2</sub> and Ar has been measured at supercritical temperature 298.15 K up to pressures of 50 MPa using the gravimetric method.

When the adsorption equilibria of gases on the surface of solids are measured gravimetrically, the results are highly accurate, reproducible and obtain a better resolution and accuracy than when volumetric measuring methods are applied. In order to take advantage of the gravimetric measuring principle a magnetic suspension balance has been designed and built which allows adsorption measurements to be carried out in the pressure range from vacuum to 50 MPa.

In this paper, the experimental installation and the measuring procedure are explained. After this the handling (i.e. analyzing procedure) of the experimental data is described. The results of this procedure are the

properties of the adsorbent, of the adsorbed phase and the adsorption equilibria data. These will be analyzed and, to a certain extent, discussed.

## Experimental

The measuring installation for the gravimetric investigation of adsorption equilibria in the pressure range from vacuum to 50 MPa at temperatures between 290 K and 500 K was designed and produced by Rubotherm Präzisionsmeßtechnik GmbH (Bochum, Germany). A brief description of the instruments with their working principles and accuracy is given below. After this the measuring process and the experimental materials used are described.

### Gravimetric Measurement

The main part of the experimental installation is the magnetic suspension balance. This type of instrument allows the elimination of most of the disadvantages of the gravimetric technique by physically separating the high resolution balance and the sample under investigation: The sample is exposed to the measuring

atmosphere while the balance is located under ambient conditions. This is achieved by using a magnetic suspension coupling, shown in Fig. 1, which transmits the force acting on the sample due to gravity through the wall of a pressure and temperature resistant vessel to the high resolution balance located outside the vessel (Gast, 1978; Lösch et al., 1994, 1995).

Using this measuring principle a broad range of standardized gravimetric instruments with a magnetic suspension balance have been developed. Among these are instruments for the measurement of sorption processes and equilibria (Dreisbach et al., 1996, 1999; Pfannschmidt and Michaeli, 1998; Frère et al., 1999; De Weireld et al., 1999b), for thermogravimetric measurements (Stolle and Wahl, 1995; Arndt et al., 1995) and for the measurement of the density of gases and liquids (Pieperbeck et al., 1991; Wagner et al., 1995; Masuda et al., 1998). In this study the so-called "Universal Sorption Measuring Apparatus" shown in Fig. 2 has been used. This instrument allows sorption measurements to be carried out with almost any pure or mixed gas or liquid in the pressure range from ultra high vacuum to 500 bar at temperatures between 270 K and 500 K.

High resolution (0.01 mg) gravimetric measurements in this range of applicability can be performed by

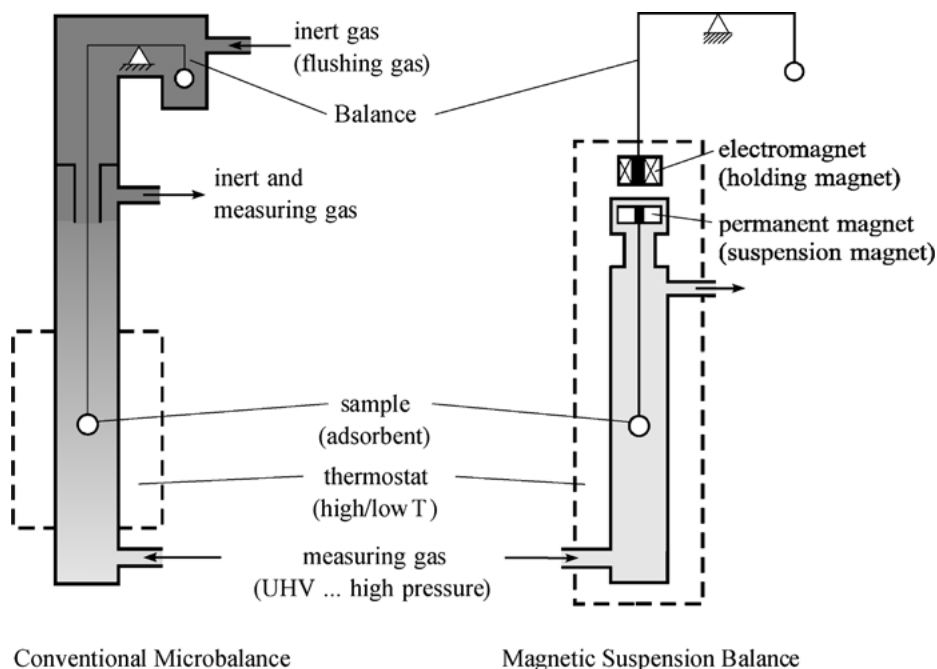


Figure 1. Gravimetric measurements under controlled environments: Comparison of conventional instrument (left) and magnetic suspension balance (right).

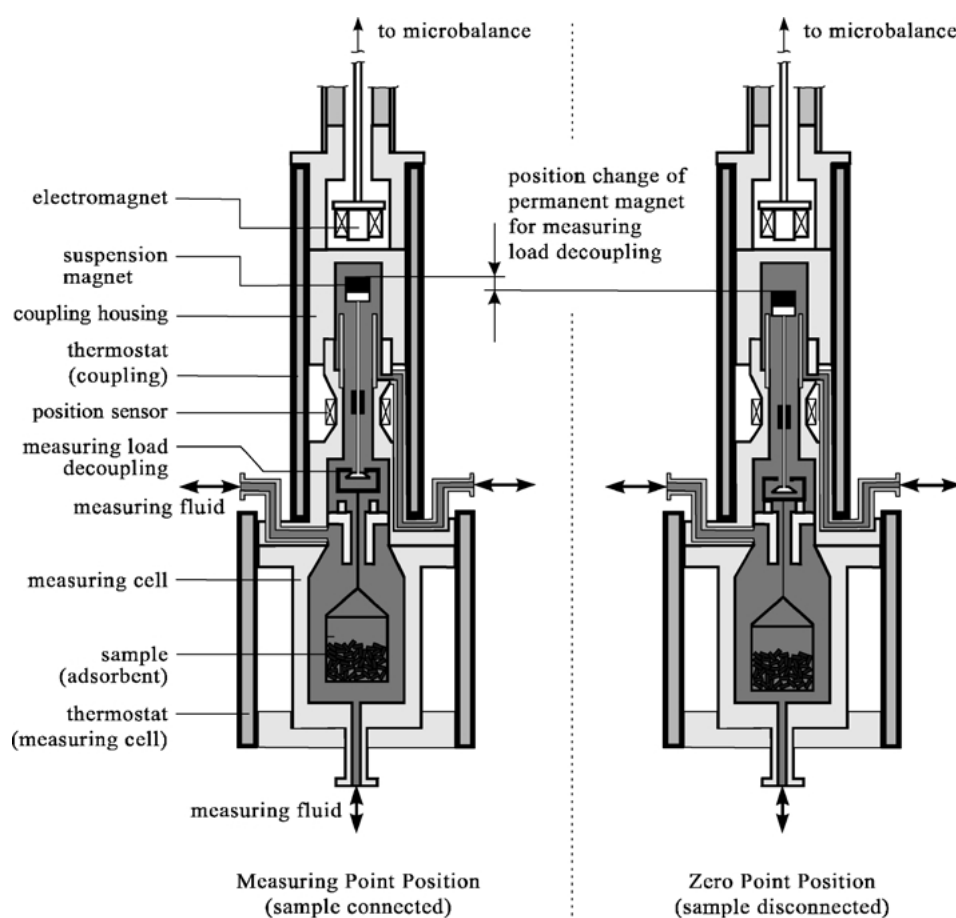


Figure 2. Universal sorption measuring apparatus with a magnetic suspension balance. Measuring position with sample connected to the balance (left) and zero point position with disconnected sample for taring and calibrating the balance (right).

separating the microbalance (Mettler AT261, Mettler, Switzerland) from the measuring atmosphere by means of a magnetic suspension coupling. This coupling consists of an electromagnet, hanging at the underfloor weighing hook of a microbalance located outside the measuring cell, and a suspension (permanent) magnet inside the measuring cell to which the adsorbent is connected. The electromagnet voltage is modulated by a controlling unit in such a way that the suspension magnet and the connected sample achieve a constant vertical position in the measuring cell. In this position the magnet and the sample are freely suspended and their mass is transmitted to the microbalance through the wall of the metal pressure vessel. Sorption processes on almost all types of samples (e.g. powders, pellets, liquids, polymers) with masses up to 40 g can be investigated in the above mentioned pressure and temperature range with high reproducibility ( $\pm 0.015$  mg).

The so-called measuring load decoupling allows the sample to be set down on a support by varying the vertical position of the permanent magnet by means of the controlling unit. When the sample is set down in the so-called "Zero Point Position" only the permanent magnet is in suspension and only its mass is transmitted to the balance. In this position the balance can be calibrated and tared. This feature enhances the accuracy of the measurements considerably. For example, it allows the buoyancy change acting on the permanent magnet to be measured separately and the measured data to be corrected even after changing the atmospheric conditions (e.g. increase in pressure). The measuring cell and the coupling area are enclosed by thermostats in order to control the temperature of the measuring gas and the sample (cp. Fig. 2). For the measuring temperatures of this study the thermostating fluid (e.g. water or oil) is circulated at a certain temperature through

double walled tubes. For measurements at higher temperatures electrical heat can be applied instead of using circulating fluid thermostats.

#### *Pressure Measurement*

Pressure in the measuring cell is measured with a piezo-resistive pressure transducer with stainless steel diaphragm (type 4090, Kistler, Switzerland). The measuring reproducibility is  $<\pm 0.1\%$  and the linearity  $<\pm 0.25\%$  FSO at operating conditions  $p \leq 50$  MPa in the temperature range from 270 K to 570 K.

#### *Temperature Measurement*

Temperature is measured in the measuring cell just below the adsorbent sample with a Pt100 temperature probe (1/10 DIN IEC751 class B, Merz, Germany). Accuracy of the temperature measurement is  $<\pm 0.05$  K at temperatures below 370 K.

#### *Pressurizing the Measuring Gas*

Since the gas cylinders normally used for the supply of the measuring gas provide a maximum pressure of 20 MPa the gas needs to be compressed for adsorption measurements at higher pressures. For this purpose a pneumatic driven compressor (type AG, Haskel, USA) is applied, which reaches the desired end pressure of 50 MPa easily if the feed gas is provided at pressures not below 2 MPa.

#### *Data Acquisition*

The data acquisition and the control of the magnetic suspension balance are performed using a personal computer and the so-called "MessPro" software (Rubotherm, Germany).

This software allows the following data to be recorded:

- (i) mass changes of the sample measured with the magnetic suspension coupling,
- (ii) pressure of the measuring gas measured with the pressure transducer,
- (iii) temperature in the measuring cell measured with the Pt100 thermometer.

In addition all measured values as a function of time are displayed online on the PC screen. This visualization

means that the status of the measurement process can be easily revised by the user, for example the approach of the adsorption equilibrium which is identified by constant values of measured mass, pressure and temperature.

The software controls the magnetic suspension balance. This means that the changes between measuring the sample mass (Measuring Point Position) and weighing only the permanent magnet (Zero Point Position) are performed periodically by the software. The data in both positions are recorded and used to correct the drift of the microbalance and the buoyancy acting on the permanent magnet.

#### *Adsorption Measurements*

As adsorbent for the measurements of this work the microporous activated carbon (AC) Norit R1 provided from Norit B.V. (The Netherlands) was used. The specific surface area of the AC was measured with  $N_2$  at 77 K applying the BET method and found to be  $1417 \text{ m}^2/\text{g}$  (Gregg, 1967). The specific micropore volume was calculated according to the method of Horvath and Kawazoe based on adsorption data of Ar at 87 K and found to be  $0.63 \text{ cm}^3/\text{g}$ . As adsorptive gases in this work  $CH_4$ ,  $N_2$  and Ar were used. Helium was used as flushing gas during the reactivation of the adsorbent and for measuring the specific volume of the activated carbon. All gases were supplied with a purity of more than 99.995%.

Carrying out an adsorption measurement with a gas at one temperature (here 298.15 K) involves three steps:

1. The sample container is filled with the adsorbent which is then weighed with the magnetic suspension balance.
2. The adsorbent material is reactivated, i.e. the measuring cell is evacuated several times and flushed with Helium. After this, the measuring cell is filled with He up to a certain pressure (1 MPa) and heated up to at least 350 K and held at this temperature for 1 hour. Next, the cell is evacuated and cooled down to the measuring temperature. After reaching equilibrium, i.e. at the end pressure of evacuation ( $<1$  Pa) and at measuring temperature when the mass of the sample is constant, the mass of the activated sample is weighed with the magnetic suspension balance. During this procedure the mass changes of the sample are continuously monitored by the magnetic suspension balance.

3. The measuring cell is pressurized with the desired measuring gas (He, CH<sub>4</sub>, N<sub>2</sub>, Ar) and the process of equilibration observed with the magnetic suspension balance. After the adsorption equilibrium is reached and all relevant measures (pressure  $p$ , temperature  $T$ , and balance signal  $\Delta m$ ) have been recorded the pressure is increased to the next desired value. This carries on until the maximum pressure of the isotherm is reached (here 50 MPa).

After measuring the last point of the isotherm the pressure is either reduced stepwise and the desorption isotherm measured or the measuring cell is emptied and evacuated without measuring the desorption branch. The next isotherm can be initiated by reactivating the adsorbent again or by filling the sample container with a new sample material as described above.

### Data Analysis

Several previous publications have shown (Sircar, 1985; Staudt et al., 1993; Myers et al., 1997) that the commonly used measuring techniques for adsorption equilibria allow only differences to be measured, i.e. the mass of adsorbate minus the product of the volume of the atmosphere displaced by the adsorbent and the density of the atmosphere surrounding it. This is valid for the volumetric method (dead volume) and for the gravimetric method (buoyancy). There are two sensitive points:

1. The volume of a highly porous solid (which adsorbents usually are) cannot be measured absolutely, i.e. they do not have a value independent of measuring technique. The volume can only be approximated using a measuring technique with Helium as adsorptive gas, assuming Helium is not adsorbed and can reach the same range of pores as the adsorptive gas does (assuming no size exclusion) (Gregg, 1967; Young and Crowell, 1962). Both assumptions have been proven wrong and found to be invalid in some cases (Kaneko, 1992; Staudt et al., 1997; Robens et al., 1999). Recent publications indicate that Helium adsorption occurs even at high temperatures and medium pressures and should not be ignored in the correction of the experimental data (Sircar, 2001).
2. Up to now the volume of the adsorbed molecules has usually been neglected. This is valid only for the calculation of the surface excess adsorbed

following the Gibbs definition. Absolute adsorption can be derived from measured data by assuming the adsorbate has a volume (Myers et al., 1997; Keller et al., 1999; Dreisbach et al., 1999). This volume has always been estimated by assuming the adsorbate has liquid density (Dreisbach et al., 1999). We will show later on that this assumption cannot be applied to adsorption data at high pressures.

Focusing now on the measuring situation in gravimetric experiments with a magnetic suspension balance: the measured quantities are the balance reading ( $\Delta m$ ), pressure ( $p$ ) and temperature ( $T$ ). Due to the buoyancy effects acting on the adsorbent and the components of the balance holding the sample this measure is equal to the difference:

$$\Delta m(p, T) = m(p, T) - [V + V_{SC}] \cdot \rho(p, T) \quad (1)$$

In this equation the quantity  $V_{SC}$  is characteristic for the balance;  $V_{SC}$  is the volume of the balance components holding the sample. These numerical values are not dependent on the pressure and can be measured in a calibration experiment with an empty balance. Introducing this volume in Eq. (1) allows the derivation of the so-called reduced mass of adsorbate  $\Omega$  from the measured data:

$$\begin{aligned} \Omega(p, T) &= \Delta m(p, T) + V_{SC} \cdot \rho(p, T) \\ &= m(p, T) - V \cdot \rho(p, T) \end{aligned} \quad (2)$$

where  $\Delta m$  is the reading of the balance,  $\rho(p, T)$  the density of the atmosphere surrounding the sample and  $V$  the volume of the adsorbent sample displacing the atmosphere.

To obtain the quantity of interest, the mass of adsorbate  $m$  from the measured data, a buoyancy correction obviously has to be performed:

$$\begin{aligned} m(p, T) &= \Omega(p, T) + V \cdot \rho(p, T) \\ &= \Delta m(p, T) + (V_{SC} + V) \cdot \rho(p, T) \end{aligned} \quad (3)$$

Equation (3) can be used with different “physical philosophies” to derive either

- (i) the surface excess adsorbed. Here  $V$  characterizes only the volume of the adsorbent, or
- (ii) the absolute adsorption. Here  $V$  is the volume of the adsorbent and the adsorbate displacing the gas phase and causing the buoyancy effect.

We focus now on the latter and present a modification of the model for the volume of the adsorbed phase which leads to an improvement in the data handling procedure.

### Volume Model

The volume  $V$  characteristic for the system adsorbent and adsorbate consists of two parts:

$$V = V_{AC} + V_{ADS} = V_{AC} + \frac{m}{\rho_{ADS}} \quad (4)$$

The first part is the volume of the activated carbon adsorbent  $V_{AC}$ , which following the classical technique has been measured with Helium. The second part is the volume of the adsorbed molecules  $V_{ADS}$ . This is defined by dividing the adsorbed mass,  $m$  by the density of the adsorbed phase,  $\rho_{ADS}$ . In this paper the density of the adsorbed phase is assumed not to be constant but to be compressible and pressure dependent.

### Helium Volume

In order to obtain a value for the volume of the activated carbon the so-called Helium-volume was determined. Therefore, we performed measurements with He as adsorptive gas: In a first measurement the empty balance was pressurized with He for the determination of the volume  $V_{SC}$  of the balance parts causing buoyancy. In a second measurement reactivated AC Norit R1 was used as a sample on the balance and, similar to the measurements with the empty balance, pressurized with He up to 50 MPa. Applying Eq. (3) with the assumption that He is not adsorbed at all ( $m = m_{He}(p, T) = 0$ ) the so-called Helium volume of the AC can be calculated from the measured data. Its values are shown in Fig. 3 as a function of the pressure of the gas phase.

The error bars at the measured volume values are, on the whole, defined by the uncertainty of the pressure measurement at low pressures (calculation of the gas phase density  $\rho = \rho(p, T)$ ). It is obvious from Fig. 3 that the Helium-volume of the AC Norit R1 is not independent of the pressure. At higher pressures, where the uncertainty of the measurement is small, the specific volume definitely increases.

By analyzing Fig. 3 it can be verified that the increase of the measured volume  $V_{AC}$  is only caused by the activated carbon! For this purpose the results of calibration measurements for the determination of the volume of

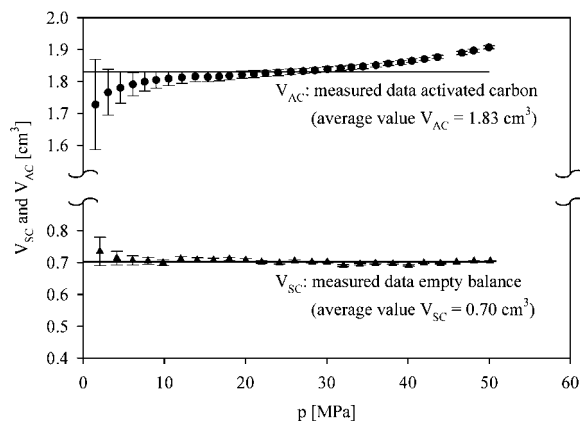


Figure 3. Volumes measured using Helium as adsorptive gas at  $T = 298.15$  K: upper symbols (●): balance loaded with activated carbon; Lower symbols (▲): empty balance.

the balance components (empty balance), which have been performed with Helium at the same temperature and the same pressure range, are also shown in Fig. 3. Obviously the volume of the empty balance is independent of the Helium pressure. From this the conclusion can be drawn, that the observed volume increase of the adsorbent is assumed to be:

- either a systematic error in the volume determination due to the adsorption of Helium which occurs but neglected in the data analysis or
- a real swelling of the activated carbon as a result of Helium being absorbed in the lattice of the activated carbon or
- both effects together.

The fact that activated carbon definitely does not behave inertly towards Helium, i.e. ad- or absorption occurs even at room temperature and low pressures, has been verified elsewhere (Staudt et al., 1997). Recently a method to correct of the influence of the Helium adsorption on the volume determination of adsorbent material was proposed (Sircar, 2001), in which a second measurement with Helium has to be performed using a chemically inert and low surface area material with the same density as the real adsorbent. By comparing this measurement with the Helium measurement performed with the adsorbent, the amount of Helium adsorbed can be estimated and corrected. For the measurements of this work the proposed method could not be used, since the application of this method is limited to adsorbent materials of which the density is known from independent methods (e.g. crystallography). In

the case of activated carbon this is not possible. Here the density is usually measured itself with Helium and thus, incorrect.

For the buoyancy correction of the measured adsorption data of the gases CH<sub>4</sub>, N<sub>2</sub>, and Ar a pressure independent average value  $V_{AC}$  of the measured volumes is used (specific Helium-volume used:  $v_{He} = 0.447 \text{ cm}^3/\text{g}$ ). This pressure independent value was chosen because the observed swelling behavior is assumed to be a “Helium effect”. This means, the swelling does not necessarily occur during the adsorption of the other gases since their larger molecules may not be able to penetrate the activated carbon lattice. Even if one presumes that the swelling of the adsorbent material also occurs during the adsorption of the other gases, the slope of the pressure dependence of the volume cannot be transferred easily from Helium to other gases.

#### Adsorbate Volume

In order to calculate the absolute adsorption from measured data the volume of the adsorbed phase has to taken into account in the buoyancy correction. Several suggestions for the estimation of this volume have been made during the last years (Staudt et al., 1993; Dreisbach et al., 1999). Here one of them is briefly discussed whereby the density of the adsorbed phase is assumed to be the liquid density in a reference state (boiling point at 1 atm) (Dreisbach et al., 1999). This assumption allows the physically reasonable correction of gravimetric and volumetric measured adsorption data in the pressure range up to 6 MPa. In this context physically reasonable behavior for absolute adsorbed mass  $m$  means (Keller et al., 1999):

$$\left(\frac{\partial m}{\partial p}\right)_T \geq 0 \quad (5)$$

i.e. the adsorbate mass must increase or have a limiting, constant value with increasing pressure (at a constant temperature). A decrease with increasing pressure is not possible for absolute adsorbed mass.

Due to the lack of adsorption data at higher pressures the practicability of this model could not be proven extensively. Using the data of this work this model was checked and found to deliver physically reasonable results up to certain, adsorptive dependent pressures (13.5 MPa for CH<sub>4</sub>, 21 MPa for N<sub>2</sub> and 23.5 MPa for Ar), but not above. For this reason, we conclude that

the density of the adsorbed phase cannot be the liquid density.

Therefore we propose an other technique for the estimation of the density of the adsorbed phase, which is a further development of a model proposed in the publication (Staudt et al., 1993). The unknown density of the adsorbed phase is treated as a parameter of an analytical model, which is used to represent the experimental data. The buoyancy causing volume of the adsorbent and adsorbate is the sum of the adsorbent volume  $V_{AC}$  (Helium-volume) and the adsorbate volume  $V_{ADS}$  (cp. Eq. (4)). The experimental data  $\Omega(p, T)$  (cp. Eq. (2)) can be represented by the analytical isotherm  $m_{ANA}$  (cp. Eqs. (7), (9) and (11) below) and the volume model Eq. (4) in the following way:

$$\begin{aligned} \Omega(p, T) &= m_{ANA}(p, T) - V \cdot \rho(p, T) \\ &= m_{ANA}(p, T) - \left( V_{AC} + \frac{m}{\rho_{ADS}} \right) \cdot \rho(p, T) \end{aligned} \quad (6)$$

Here  $m_{ANA}(p, T)$  is an analytical function for the adsorption isotherm. The parameters of this analytical adsorption isotherm are fitted together with the unknown density of the adsorbate,  $\rho_{ADS}$  to the experimental data by a least square optimization.

Obviously the resulting parameters depend on the analytical function,  $m_{ANA}(p, T)$  which is chosen to describe the data. However, the density of the adsorbed phase  $\rho_{ADS}$  is a physical property and must not be dependent on the analytical model but should have the same value for different models. In order to prove this independency and therefore the applicability of the proposed data treatment three different analytical isotherms have been used for the fitting procedure.

#### Analytical Isotherm Model

The three analytical isotherms used for the representation of the data in this work are isotherms which are able to describe data of the IUPAC type I. These isotherms were chosen since the adsorption of the supercritical gases CH<sub>4</sub>, N<sub>2</sub> and AR on the microporous AC is expected to be of IUPAC type I (Sing et al., 1985).

Density has been used as a variable in the isotherms instead of using pressure simply because there are some practical advantages in the parameter optimization procedure.

*Langmuir Isotherm*

The first analytical isotherm used for the representation of the data in this work is a Langmuir isotherm with so-called fractal exponents  $\alpha$ . The exponents  $\alpha$  allow the range of applicability of the analytical model in pressure/density to be extended (Keller, 1990):

$$m_{\text{ANA,LANGMUIR}} = m_{\infty} \cdot \alpha \cdot \frac{(b \cdot \rho(p, T))^{\alpha}}{1 + (b \cdot \rho(p, T))^{\alpha}} \quad (7)$$

Introducing this isotherm in Eq. (6) leads to the parameter optimization function for the Langmuir isotherm as:

$$\Omega(p, T) = m_{\infty} \cdot \alpha \cdot \frac{\{b \cdot \rho(p, T)\}^{\alpha}}{1 + \{b \cdot \rho(p, T)\}^{\alpha}} - \left( V_{\text{AC}} + \frac{m}{\rho_{\text{ADS}}} \right) \cdot \rho(p, T) \quad (8)$$

The numerical values of the four parameters of the model (i.e.  $m_{\infty}$ ,  $b$ ,  $\alpha$  for the isotherm and  $\rho_{\text{ADS}}$  for the adsorbate) are determined by a least square fitting procedure.

*Toth Isotherm*

The second analytical isotherm used for the representation of the data is the Toth isotherm. This isotherm model is chosen, since it takes the energetically heterogeneity of the AC into account, assumes a type I adsorption and is widely used (Toth, 1984):

$$m_{\text{ANA,TOTH}} = m_{\infty} \cdot \frac{\rho(p, T)}{\left(\frac{1}{b} + \rho(p, T)\right)^{1/\alpha}} \quad (9)$$

Introducing this isotherm in Eq. (6) leads to the parameter optimization function for the Toth isotherm as:

$$\Omega(p, T) = m_{\infty} \cdot \frac{\rho(p, T)}{\left(\frac{1}{b} + \rho(p, T)\right)^{1/\alpha}} - \left( V_{\text{AC}} + \frac{m}{\rho_{\text{ADS}}} \right) \cdot \rho(p, T) \quad (10)$$

The numerical values of the four parameters of the model (i.e.  $m_{\infty}$ ,  $b$ ,  $\alpha$  for the isotherm and  $\rho_{\text{ADS}}$  for the adsorbate) are determined by a least square fitting procedure.

*UNILAN Isotherm*

The third analytical isotherm used is the UNILAN isotherm. The UNILAN model is an empirical relation which accounts for heterogeneity by assuming patch-wise topography on the surface with ideal patches, so that a local Langmuir isotherm is applicable on each patch (Do, 1998):

$$m_{\text{ANA,UNILAN}} = \frac{m_{\infty}}{2 \cdot \alpha} \cdot \ln \left[ \frac{1 + b \cdot e^{\alpha} \cdot \rho(p, T)}{1 + b \cdot e^{-\alpha} \cdot \rho(p, T)} \right] \quad (11)$$

Introducing this isotherm in Eq. (6) leads to the parameter optimization function for the Langmuir isotherm as:

$$\Omega(p, T) = \frac{m_{\infty}}{2 \cdot \alpha} \cdot \ln \left[ \frac{1 + b \cdot e^{\alpha} \cdot \rho(p, T)}{1 + b \cdot e^{-\alpha} \cdot \rho(p, T)} \right] - \left( V_{\text{AC}} + \frac{m}{\rho_{\text{ADS}}} \right) \cdot \rho(p, T) \quad (12)$$

The numerical values of the four parameters of the model (i.e.  $m_{\infty}$ ,  $b$ ,  $\alpha$  for the isotherm and  $\rho_{\text{ADS}}$  for the adsorbate) are determined by a least square fitting procedure.

**Data Fit**

In order to investigate the reliability of the models proposed above and to decide whether the density of the adsorbed phase is constant or a function of the adsorptive pressure or the chosen adsorption isotherm, the parameter optimization procedure was performed five times for each individual isotherm model and gas. The distinguishing feature between the optimizations were the experimental data used. One run was performed using all data, for the others only data up to a certain maximum pressure were used. The maximum pressures for the four runs were chosen to be: 40 MPa, 30 MPa, 20 MPa and 10 MPa. Thus, the resulting five sets of parameters, especially the fitted density of the adsorbed phase, are characteristic for isothermal data up to a certain pressure.

The fittings were performed using the spreadsheet software SigmaPlot2000. Resulting parameter values as well as the corrected adsorption data for the gases CH<sub>4</sub>, N<sub>2</sub>, and Ar on the AC Norit R1 are presented and discussed in the next section of this paper.



## Results

### Adsorbate Density

The four parameters of each model (i.e.  $m_\infty$ ,  $b$ ,  $\alpha$  for the isotherm and  $\rho_{\text{ADS}}$  for the adsorbate) were determined by a least square fitting procedure for each gas five times. The data used for each individual parameter optimization are distinguished by the pressure range covered, vac.-50 MPa, vac.-40 MPa, vac.-30 MPa, vac.-20 MPa, and vac.-10 MPa. As an example in the following Tables 1–3 the parameter sets resulting from the fitting for  $\text{CH}_4$  are compared. In each table the parameters for one analytical isotherm are given. For the other gases under investigation very similar parameter sets were found.

The changes in the parameters of the isotherm due to the maximum pressure of the data used for the optimization procedure are strongly systematic. The isotherm parameter limiting load ( $m_\infty$ ), i.e. the mass

adsorbed at infinite pressure, slightly increases for all three models if only data from lower pressures are used. In the case of the Langmuir isotherm used (cp. Table 1) not the quantity  $m_\infty$  alone but the product of the parameters  $m_\infty$  and  $\alpha$  is the so-called limiting loading of the isotherm. The observed increase is reasonable, since the measured data in the lower pressure regime (used for the optimization) belong moreover to the increasing branch of the isotherm. The more the high pressure data are taken into account for the optimization, the “clearer” the plateau of the isotherm appears and the better the limiting value is defined.

The parameter  $b$  is a measure for the adsorption affinity in all three isotherm models used (in the case of the Toth isotherm it is  $b^{1/\alpha}$ ). It is in general defined by the slope of the isotherm at low pressures and should remain almost unchanged whether or not highest pressure data are used. Exactly this behavior can be observed from the Tables 1–3 for all three isotherms used. In all three models the parameter  $\alpha$  represents

Table 1. Parameters of the Langmuir-isotherm and the density of the adsorbed phase resulting from parameter optimizations of experimental  $\text{CH}_4$  data up to different maximum pressures (Eq. (7)).

	$p_{\text{max}} = 50 \text{ MPa}$	$p_{\text{max}} = 40 \text{ MPa}$	$p_{\text{max}} = 30 \text{ MPa}$	$p_{\text{max}} = 20 \text{ MPa}$	$p_{\text{max}} = 10 \text{ MPa}$
$m_\infty$ (mg/g)	182.61	200.78	221.12	240.81	238.33
$b$ ( $\text{dm}^3/\text{g}$ )	0.11	0.10	0.09	0.08	0.08
$\alpha$ (–)	0.83	0.79	0.75	0.72	0.72
$\rho_{\text{ADS}}$ ( $\text{g}/\text{dm}^3$ )	376.42	364.63	352.15	338.77	345.86
$m_\infty \cdot \alpha$ (mg/g)	151.57	158.61	165.84	173.38	171.60

Table 2. Parameters of the Toth isotherm and the density of the adsorbed phase resulting from parameter optimizations of experimental  $\text{CH}_4$  data up to different maximum pressures (Eq. (9)).

	$p_{\text{max}} = 50 \text{ MPa}$	$p_{\text{max}} = 40 \text{ MPa}$	$p_{\text{max}} = 30 \text{ MPa}$	$p_{\text{max}} = 20 \text{ MPa}$	$p_{\text{max}} = 10 \text{ MPa}$
$m_\infty$ (mg/g)	154.37	163.37	175.01	190.09	193.70
$b$ [ $(\text{dm}^3/\text{g})^\alpha$ ]	0.27	0.32	0.37	0.43	0.44
$\alpha$ (–)	0.77	0.70	0.63	0.57	0.55
$\rho_{\text{ADS}}$ ( $\text{g}/\text{dm}^3$ )	375.85	363.11	348.96	331.59	335.75
$b^{1/\alpha}$ ( $\text{dm}^3/\text{g}$ )	0.18	0.20	0.21	0.23	0.22

Table 3. Parameters of the UNILAN isotherm and the density of the adsorbed phase resulting from parameter optimizations of experimental  $\text{CH}_4$  data up to different maximum pressures (Eq. (11)).

	$p_{\text{max}} = 50 \text{ MPa}$	$p_{\text{max}} = 40 \text{ MPa}$	$p_{\text{max}} = 30 \text{ MPa}$	$p_{\text{max}} = 20 \text{ MPa}$	$p_{\text{max}} = 10 \text{ MPa}$
$m_\infty$ (mg/g)	149.74	155.16	161.94	171.59	175.90
$b$ ( $\text{dm}^3/\text{g}$ )	0.12	0.11	0.10	0.08	0.08
$\alpha$ (–)	1.53	1.76	2.00	2.25	2.35
$\rho_{\text{ADS}}$ ( $\text{g}/\text{dm}^3$ )	377.14	365.53	352.52	335.28	333.24

the energetic heterogeneity of the system but is defined in a different way. For the Langmuir and the Toth isotherm the heterogeneity increases if  $\alpha$  increases. In the UNILAN isotherm the parameter  $\alpha$  decreases with increasing heterogeneity. For all three isotherms an increase in heterogeneity is observed with increasing pressure. The heterogeneity of the system is a measure for the difference of the interaction energies of sites occupied. At low pressures first the “high” energy sites are occupied, with increasing pressure the “lower” energy sites are then occupied and thus, the heterogeneity of the system should increase with increasing pressure.

Notably, the change of the density of the adsorbed phase is surprisingly systematic and uniform for all isotherm models used. With increasing pressure of the adsorptive gas the density of the adsorbed phase increases almost linearly. The correlation between the optimized density values and the pressure is visualized in Fig. 4 for all three gases and all three isotherm models under investigation. For each gas the density values determined with each of the three isotherm models are shown—the resulting symbols almost lie on each other and show no deviation.

From Fig. 4 it is obvious, that for all three gases the densities of the adsorbed phase, determined by the optimization procedure described above, are linear functions of the gas phase pressure and independent of the isotherm model used. This is valid for all calculations using experimental data with maximum pressures of 20 MPa and above (in Fig. 4 indicated as framed symbols). The density value for maximum pressure of

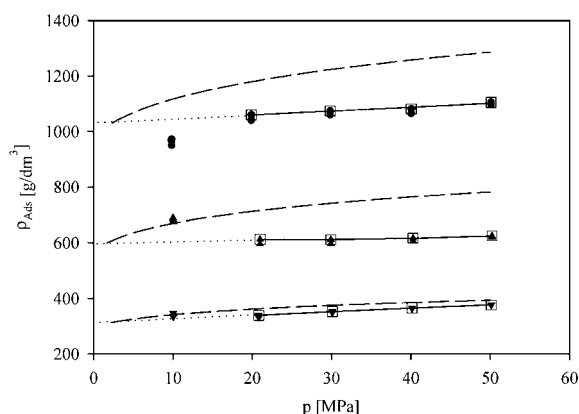


Figure 4. Adsorbed phase densities determined from data fit with three different isotherm models up to certain pressures. ( $\nabla$ ):  $\text{CH}_4$ ; ( $\blacktriangle$ ):  $\text{N}_2$ ; ( $\bullet$ ): Ar. Dashed lines are densities of compressed free liquid calculated according to Reid (1989).

10 MPa does not fit in this linear dependency for all three gases. A reason for this may be the small number of data belonging to the “buoyancy related” decreasing branch of the isotherm at this pressure.

In Fig. 4 the isothermal densities of compressed liquids are given as a function of the pressure (dashed lines). The compressed liquid densities have been calculated for the three substances  $\text{CH}_4$ ,  $\text{N}_2$  and Ar with the algorithm and the parameters given in literature (Reid et al., 1989, pp. 55–66). The temperatures belonging to these isotherms have been chosen in such a way, that the “zero pressure” density of the adsorbate (linearly extrapolating the fitted densities to low pressures, cp. the dotted lines in Fig. 4) is equal to the liquid density at that temperature. Obviously, both the densities and the compressibilities of the free liquids in phase equilibrium with vapor are in the same order of magnitude as the fitted density values of the adsorbate. The calculated densities of the compressed free liquids show systematically 20% higher values than the fitted densities of the adsorbed phase. This is valid for all three gases under investigation. This systematic behavior indicates the physical sensibility of the model used and the parameters as well as the performance of the fitting procedure. Moreover, the “zero pressure” density for all three gases was found to be exactly 1.92 times the critical density! If this systematic behavior is also true for other adsorbents and/or at other temperatures has to be investigated in further experiments.

In Fig. 5 the volumes of the adsorbent-adsorbate system, calculated according to Eq. (4) with the density of the adsorbed phase shown in Fig. 4, are given as a

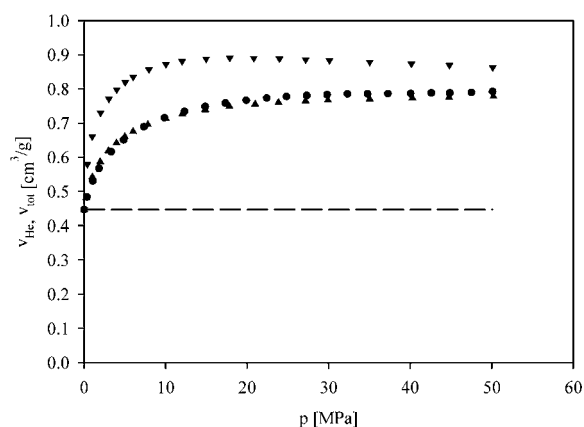


Figure 5. Volume of the adsorbent (AC Norit R1) and the adsorbed phase. ( $\nabla$ ):  $\text{CH}_4$ ; ( $\blacktriangle$ ):  $\text{N}_2$ ; ( $\bullet$ ): Ar. Dashed line is the specific volume of the adsorbent measured with Helium.

function of the gas phase pressure. The starting value in vacuum is the volume of the reactivated adsorbent for all three adsorptives. This is approximated with the measured Helium volume. It is obvious from Fig. 5 that for all three adsorptives under investigation the volume of the adsorbed phase is almost in the same order of magnitude as the volume of the adsorbent.

It is interesting to note, that the resulting volumes for  $N_2$  and Ar are almost equal to each other and show a continuous increase with the pressure of the gas phase. The volume resulting for  $CH_4$  does not grow continuously but shows a maximum at a gas phase pressure of 20 MPa and at higher pressures a decrease. This indicates, that the compressibility of the adsorbed phase for  $CH_4$  is larger than the increase of its volume by the additional adsorption of new molecules.

### Adsorption Data

Using the model described above and the fitted parameters for the density of the adsorbed phase, the buoyancy correction of the gravimetrically measured adsorption data may be performed. In the Figs. 6–8 the resulting adsorption isotherms are shown. In these Figures the following information is given:

- the experimental data (reduced mass of adsorbate  $\Omega$ , cp. Eq. (2)) without any correction,
- the surface excess mass adsorbed,  $m_{ex}$  which has been calculated from the experimental data by a buoyancy correction with the Helium-volume ( $m_{ex} = \Omega + \rho \cdot v_{He}$ ),

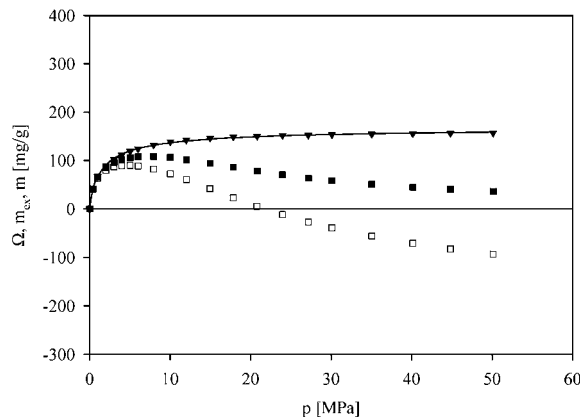


Figure 6. Adsorption equilibria of  $CH_4$  on AC Norit R1 at  $T = 298.15$  K. ( $\square$ ): exp. data (reduced mass  $\Omega$ , cp. Eq. (2)), ( $\blacksquare$ ): surface excess adsorbed (corrected with  $V_{AC} = V_{He}$ ), ( $\blacktriangledown$ ): absolute adsorption (corrected with volume cp. Eq. (4)).

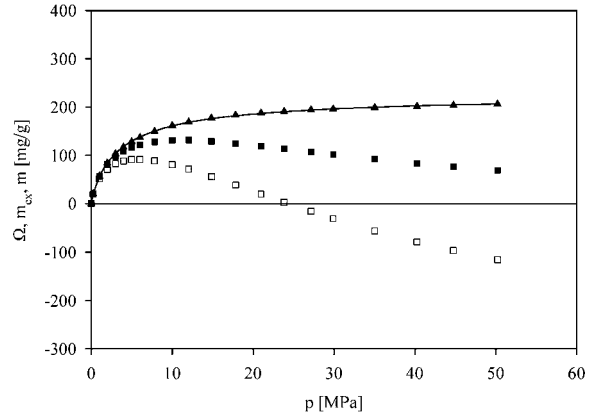


Figure 7. Adsorption equilibria of  $N_2$  on AC Norit R1 at  $T = 298.15$  K. ( $\square$ ): exp. data (reduced mass  $\Omega$ , cp. Eq. (2)), ( $\blacksquare$ ): surface excess adsorbed (corrected with  $V_{AC} = V_{He}$ ), ( $\blacktriangle$ ): absolute adsorption (corrected with volume cp. Eq. (4)).

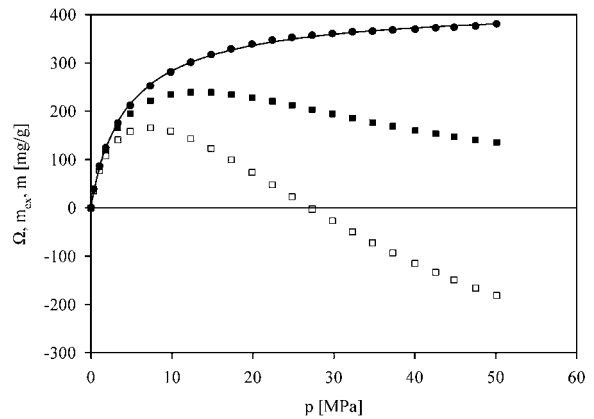


Figure 8. Adsorption equilibria of Ar on AC Norit R1 at  $T = 298.15$  K. ( $\square$ ): exp. data (reduced mass  $\Omega$ , cp. Eq. (2)), ( $\blacksquare$ ): surface excess adsorbed (corrected with  $V_{AC} = V_{He}$ ), ( $\bullet$ ): absolute adsorption (corrected with volume cp. Eq. (4)).

- the absolute adsorbed mass,  $m$  which has been calculated from the experimental data by a buoyancy correction using the adsorptive and pressure dependent volume given in Fig. 5,
- and the fitting with the generalized Langmuir isotherm model given in Eq. (7).

By analyzing the Figures the same behavior for all three adsorptive gases under investigation can be observed:

The experimental data (i.e. reduced mass  $\Omega$ ) which can be obtained from the balance reading without a buoyancy correction for either the adsorbent or the adsorbate, show a steep increase at low pressures. In this part of the isotherm the increasing adsorption

dominates over the buoyancy effect. At pressures above 6 MPa the buoyancy dominates, which leads to a decrease of the reduced masses of adsorbate. For all three gases this quantity becomes even negative at pressures above 20 MPa–30 MPa, thus indicating that the buoyancy acting on the sample is larger than the mass of adsorbate.

The surface excess mass of adsorbate ( $m_{\text{ex}}$ ) shows like the experimental data an increase at low pressures where the adsorption effect dominates. At pressures larger than 10 MPa this behavior changes and the buoyancy is the dominating influence. For all three gases a decrease in the surface excess adsorbed can be noticed at higher pressures. Contrary to theory the surface excess does not approach zero as the limiting value at highest pressures, but seems to approach a constant value larger than zero. This indicates the physical imperfection of the buoyancy correction with the Helium-volume.

The absolute adsorption,  $m$  calculated with the sum of the Helium-volume of the adsorbent and the volume of the adsorbed phase shows for all three gases a typical type I behavior: a steep increase at low pressures and at higher pressures the approach to a plateau. These data can be well represented for all three gases using a fitting with the generalized isotherm of Langmuir type. The fittings are shown as a line in the Figures.

In order to allow a comparison of the adsorption capacity of the activated carbon Norit R1 for the three gases in Fig. 9 all (absolute) isotherms are shown together. Here the absolute adsorbed masses are

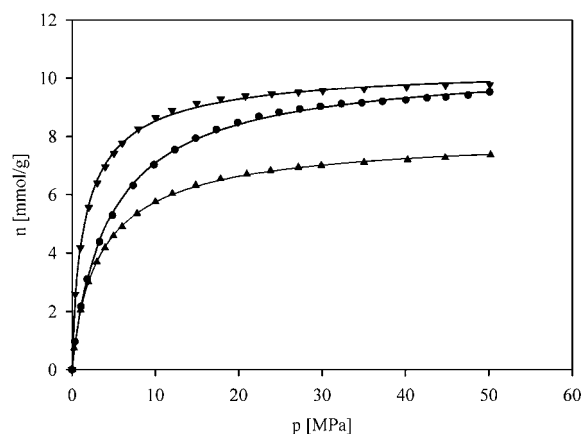


Figure 9. Adsorption equilibria of CH<sub>4</sub>, N<sub>2</sub> and Ar on AC Norit R1 at  $T = 298.15$  K. Data are given as specific amounts adsorbed in mmol/g. (▼): CH<sub>4</sub>, (▲): N<sub>2</sub>, (●): Ar, lines represent fitting of data with Langmuir isotherm Eq. (7).

converted into absolute amounts adsorbed,  $n$  in mmol/g by division of the adsorbed masses with the molar mass of the adsorptive gases. This type of presentation of adsorption data is usually used for comparison and/or calculation purposes.

The isotherms show type I behavior for all gases investigated. The largest adsorption capacity is found for CH<sub>4</sub> with almost 10 mmol/g at 50 MPa, followed by Ar with 9.5 mmol/g at this pressure. The capacity of the activated carbon for N<sub>2</sub> is the lowest of the three gases.

There is a surprisingly large adsorption capacity measured at room temperature for both N<sub>2</sub> and the noble gas Ar. This large adsorption capacity qualifies these gases as unsuitable for use as adsorptives in volume/density determination of highly porous materials instead of He, which has recently been proposed in order to overcome the obvious difficulties with Helium (Rouquerol, 1999; Keller et al., 1999).

## Conclusion and Outlook

Adsorption equilibria of the gases CH<sub>4</sub>, N<sub>2</sub> and Ar on the microporous activated carbon (AC) Norit R1 have been measured in the pressure range from vacuum up to 50 MPa at temperature 298.15 K. Measurements have been carried out gravimetrically using a magnetic suspension balance.

The volume of the adsorbent has been measured with Helium as adsorptive gas in a gravimetric experiment (from vacuum up to 50 MPa at  $T = 298.15$  K). The resulting volume for the AC was found not to be constant but to grow with increasing pressure. Since this measured effect was proven to be only dependent on the AC, and not on the measuring principle or instrument used, the growth in volume is assumed to be a swelling of the AC. The question whether this swelling is a result of ad- or absorption of Helium in the matrix of the AC could not be clarified satisfactorily. For this purpose additional measurements with Helium as adsorptive gas in this large pressure range will be performed, at other temperatures and with other adsorbent materials which are expected to be more rigid than the AC used in this study (e.g. zeolites).

The buoyancy correction of the measured data with CH<sub>4</sub>, N<sub>2</sub> and Ar as adsorptives has been carried out:

- (i) using the average value of the Helium-volumes of the adsorbent measured. The result of this is the so-called surface excess adsorbed. In the pressure

range investigated these quantities showed an increase, a maximum and, at higher pressures, a decrease. Since this behavior cannot be represented by any analytical model for adsorption equilibria available in literature (e.g. Langmuir isotherm, computer simulation of adsorption processes) the quantity of interest is the absolute adsorption. In order to determine these values from the measured data an other, physically sensible volume model was used for the buoyancy correction:

- (ii) the buoyancy related volume is assumed to be the sum of the Helium-volume and the volume of the adsorbed phase. The latter is calculated by dividing the mass of adsorbed phase with its density. Since the density of an adsorbed phase is unknown, this quantity is treated as a variable in a data fit procedure. In this procedure the variables of three analytical isotherm models (Langmuir, Toth and UNILAN) and the density of the adsorbed phase have been optimized in such a way that the measured data are represented well by the fit. The resulting densities of the adsorbed phases were independent of the isotherm model used. By using only experimental data up to certain pressures, it could be demonstrated that the fitting procedure obtains physically reasonable results which are almost independent of the upper limit of pressure. Only the resulting densities of the adsorbed phases showed a linear dependency of the upper pressure limit, which is assumed to be the compressibility of the adsorbed phase. This compressibility was proven to be in the same order of magnitude as the compressibility of a free liquid phase. Moreover, systematically for all three gases the resulting adsorbate densities are exactly 1.92 times the critical density.

These results demonstrate that the density of the adsorbed phase cannot be easily identified with the liquid density and is not independent of the pressure of the adsorptive gas. The dependence of these densities on the temperature and the adsorbent material used has to be systematically investigated further.

The adsorption equilibria data resulting from the buoyancy correction with the adsorbent and pressure/loading dependent volume showed IUPAC type I behavior. For the noble gas Ar adsorption was found to be almost as large as for CH<sub>4</sub>. N<sub>2</sub> adsorption was the weakest of the three gases under investigation. The adsorption equilibria data could be represented well with a generalized Langmuir adsorption isotherm model.

## Appendix: Tabulated Experimental Data

In this chapter the previously shown adsorption data are tabulated. In order to allow other data analyzing procedures as discussed in this paper to be performed all relevant experimental data are given. In the following tables the purely experimental quantities:

- pressure,  $p$  in MPa and
- reduced mass of adsorbate,  $\Omega$  in mg/g (cp. Eq. (2)) are given. Additionally the:
- density of gas phase  $\rho$  in kg/m<sup>3</sup> calculated with a virial EOS is listed in the tables. The data resulting from the correction of the experimental quantities using the two approaches:
- surface excess adsorbed  $m_{\text{ex}}$  in mg/g (cp. Eq. (3) calculated using the helium volume) and
- absolute adsorption  $m$  in mg/g (cp. Eq. (3) calculated using the density for the adsorbed phase resulting from the fitting procedure) are also given in the tables.

Table 4. Experimental data pressure ( $p$ ) reduced mass of adsorbate ( $\Omega$ ), gas phase density ( $\rho$ ) and calculated data surface excess adsorbed ( $m_{\text{ex}}$ ), absolute adsorption ( $m$ ) for the adsorption of CH<sub>4</sub> on AC Norit R1 at 298.15 K.

$p$ (MPa)	$\rho$ (kg/m <sup>3</sup> )	$\Omega$ (mg/g)	$m_{\text{ex}}$ (mg/g)	$m$ (mg/g)
0.39	2.54	40.050	41.187	41.523
1.00	6.59	62.778	65.723	67.130
2.01	13.47	79.492	85.515	89.330
3.03	20.67	86.722	95.962	102.662
3.99	27.67	89.498	101.869	111.580
5.04	35.58	89.826	105.733	118.992
6.02	43.19	88.395	107.703	124.474
7.95	58.77	82.130	108.404	132.512
10.03	76.26	72.044	106.137	138.588
12.01	93.27	60.365	102.060	142.573
14.96	118.38	41.310	94.230	146.447
17.85	141.66	22.806	86.134	149.016
20.80	163.33	5.089	78.106	150.532
23.96	183.99	-11.782	70.472	151.758
27.17	202.43	-26.721	63.775	152.703
30.09	217.38	-38.663	58.514	153.462
35.04	239.41	-55.942	51.086	154.504
40.14	258.75	-70.646	45.030	155.532
44.81	274.21	-82.028	40.556	156.443
50.12	289.76	-93.261	36.277	156.822

Table 5. Experimental data pressure ( $p$ ) reduced mass of adsorbate ( $\Omega$ ), gas phase density ( $\rho$ ) and calculated data surface excess adsorbed ( $m_{\text{ex}}$ ), absolute adsorption ( $m$ ) for the adsorption of  $\text{N}_2$  on AC Norit R1 at 298.15 K.

$p$ (MPa)	$\rho$ (kg/m <sup>3</sup> )	$\Omega$ (mg/g)	$m_{\text{ex}}$ (mg/g)	$m$ (mg/g)
0.24	2.71	19.408	20.621	20.714
1.02	11.54	51.183	56.344	57.447
1.97	22.33	70.965	80.947	84.069
2.99	33.93	82.391	97.560	103.390
3.97	45.06	88.309	108.455	117.228
4.99	56.61	91.134	116.441	128.513
6.00	68.02	91.613	122.022	137.533
7.82	88.45	88.639	128.179	150.170
10.00	112.57	81.042	131.365	161.397
12.03	134.50	71.543	131.672	169.243
14.85	163.98	56.117	129.422	177.308
17.83	193.62	38.530	125.088	183.465
20.98	223.00	19.594	119.284	188.028
23.84	248.04	2.919	113.803	191.522
27.16	275.05	-15.761	107.200	194.514
29.91	295.84	-30.493	101.762	196.387
35.04	331.08	-55.773	92.233	199.280
40.27	362.82	-78.754	83.443	201.754
44.77	387.27	-96.472	76.656	203.801
50.21	413.86	-115.676	69.340	206.411

Table 6. Experimental data pressure ( $p$ ) reduced mass of adsorbate ( $\Omega$ ), gas phase density ( $\rho$ ) and calculated data surface excess adsorbed ( $m_{\text{ex}}$ ), absolute adsorption ( $m$ ) for the adsorption of Ar on AC Norit R1 at 298.15 K.

$p$ (MPa)	$\rho$ (kg/m <sup>3</sup> )	$\Omega$ (mg/g)	$m_{\text{ex}}$ (mg/g)	$m$ (mg/g)
0.34	5.64	35.564	38.085	38.294
1.07	17.83	77.004	84.973	86.466
1.82	30.46	106.895	120.512	124.172
3.31	55.88	140.880	165.859	175.317
4.85	82.54	157.895	194.796	211.627
7.34	126.35	165.327	221.812	252.440
9.84	170.87	158.405	234.790	280.688
12.32	215.12	143.312	239.480	301.303
14.84	259.70	122.698	238.793	317.066
17.33	302.88	99.164	234.565	328.963
19.88	345.78	73.466	228.044	338.589
22.41	386.67	47.863	220.720	346.972
24.84	423.99	22.868	212.411	352.675
27.32	460.30	-2.329	203.446	357.148
29.81	494.73	-26.733	194.434	360.755
32.31	527.28	-49.787	185.930	364.394
34.78	557.51	-72.371	176.860	365.537
37.27	586.14	-93.174	168.857	367.811
40.05	616.06	-115.175	160.233	369.605
42.59	641.65	-133.492	153.357	372.288
44.85	663.13	-149.294	147.157	373.477
47.51	686.98	-166.241	140.869	376.279
50.11	708.91	-181.225	135.690	380.565

## Nomenclature

$b$	Parameter of the Langmuir and UNILAN isotherm (dm <sup>3</sup> /g)
$b$	Parameter of the Toth isotherm (dm <sup>3</sup> /g) <sup><math>\alpha</math></sup>
$m$	Mass of adsorbate (g, mg)
$m_{\text{ANA,LANGMUIR}}$	Mass of adsorbate calculated with the Langmuir isotherm (mg/g)
$m_{\text{ANA,TOTH}}$	Mass of adsorbate calculated with the Toth isotherm (mg/g)
$m_{\text{ANA,UNILAN}}$	Mass of adsorbate calculated with the UNILAN isotherm (mg/g)
$\Delta m$	Balance reading (g, mg)
$m_{\infty}$	Parameter of the analytical isotherms (mg/g)
$n$	Specific amount of material adsorbed (mmol/g)
$p$	Pressure (MPa)
$T$	Temperature (K)
$V$	Volume of the adsorbent & adsorbate system (cm <sup>3</sup> )
$V_{\text{AC}}$	Volume of the activated carbon (cm <sup>3</sup> )
$V_{\text{ADS}}$	Volume of the adsorbed phase (cm <sup>3</sup> )
$v_{\text{He}}$	Specific volume of the activated carbon (0.447 cm <sup>3</sup> /g)
$V_{\text{SC}}$	Volume of the empty balance parts (cm <sup>3</sup> )
$v_{\text{tot}}$	Total specific volume of the adsorbent and the adsorbate (cm <sup>3</sup> /g)
$\Omega$	Reduced mass of adsorbate (g, mg)
$\alpha$	Parameter of the Langmuir, Toth and UNILAN isotherm –
$\rho$	Density of the gaseous adsorptive (g/dm <sup>3</sup> )
$\rho_{\text{ADS}}$	Density of the adsorbed phase (g/dm <sup>3</sup> )

## References

- Arndt, J., L. Klippe, R. Stolle, and G. Wahl, "Deposition of Platinum from Bis(Acetylacetonato)Platinum(II)," *Journal de Physique IV*, **5**, 119–126 (1995).
- De Weireld, G.M. Frère, and R. Jardot, "A New Gravimetric Method for the Automated Determination of High Temperature and High Pressure Gas Adsorption Isotherms," *Measurement Science and Technology*, **10**, 117–126 (1999b).
- Do, D.D., *Adsorption Analysis: Equilibria and Kinetics*, Imperial College Press, London, 1998.
- Dreisbach, F., R. Staudt, and J.U. Keller, "Experimental Investigation of the Kinetics of Adsorption of Pure Gases and Binary Gas

- Mixtures on Activated Carbon," in *Fundamentals of Adsorption 6 (FoA6)*, F. Meunier (Ed.), pp. 1219–1224, Elsevier, Paris, 1999a.
- Dreisbach, F., R. Staudt, and J.U. Keller, "High Pressure Adsorption Data of Methane, Nitrogen, Carbon Dioxide and their Binary and Ternary Mixtures on Activated Carbon," *Adsorption*, **5**, 215–227 (1999b).
- Dreisbach, F., R. Staudt, M. Tomalla, and J.U. Keller, "Measurement of Adsorption Equilibria of Pure and Mixed Corrosive Gases: The Magnetic Suspension Balance," in *Fundamentals of Adsorption*, M.D. LeVan (Ed.), pp. 259–268, Kluwer Academic Publishers, Boston, 1996.
- Frère, M., G. De Weireld, and R. Jardot, "Adsorption Isotherms Measurements at High Pressure and High Temperature," in *Fundamentals of Adsorption 6 (FoA6)*, F. Meunier (Ed.), pp. 279–284, Elsevier, Paris, 1999.
- Gast, Th., "A New Magnetic Coupling for the Separation of Microbalance and Reaction Vessel in Experiments with Controlled Atmospheres," *Thermochimica Acta*, **24**, 247–250 (1978).
- Gregg, S.J. and K.S.W. Sing, *Adsorption, Surface Area and Porosity*, Academic Press, London, 1967.
- Kaneko, K., "Ultramicroporosity of Porous Solids by He Adsorption," in *Proceedings of the 4th Intl. Conference on Fundamentals of Adsorption*, Kyoto, Japan, T. Suzuki (Ed.), pp. 593–602, Engineering Foundation, New York, 1992.
- Keller, J.U., "Equations of State of Adsorbates with Fractal Dimension," *Physica A*, **166**, 180–192 (1990).
- Keller, J.U., F. Dreisbach, H. Rave, R. Staudt, and M. Tomalla, "Measurement of Gas Mixture Adsorption Equilibria of Natural Gas Compounds on Microporous Sorbents," *Adsorption*, **5**, 199–214 (1999).
- Lösch, H.W., R. Kleinrahm, and W. Wagner, "Neue Magnetschwebewaagen für gravimetrische Messungen in der Verfahrenstechnik," *Jahrbuch 1994 Verfahrenstechnik und Chemieingenieurwesen*, pp. 117–137, VDI-Verlag Düsseldorf, 1994.
- Lösch, H.W., J.v. Vietinghoff, W. Wagner, and R. Kleinrahm, "Magnetic Suspension Balances for Research and Industry," in *Proceedings of the 25th Conf. on Vacuum Microbalance Techniques*, Siegen, 1993, J.U. Keller and E. Robens (Eds.), p. 79, Multi-Science-Publishing, Brentwood, 1995.
- Masuda, T., T. Shigematsu, H. Sato, and K. Watanabe, "Development of a Magnetic-Suspension-Balance Apparatus for Measuring the  $p\rho T$  Properties and Vapor-Liquid-Equilibrium of Fluids," in *Proceedings of The Nineteenth Japan Symposium on Thermophysical Properties*, Fukuoka, Japan, pp. 403–406, 1998.
- Myers, A.L., J.A. Calles, and G. Calleja, "Comparison of Molecular Simulation of Adsorption with Experiment," *Adsorption*, **3**, 107–115 (1997).
- Pfannschmidt, O. and W. Michaeli, "Determination of the Solubility and Diffusivity of Gases in Polymers by Using a High Pressure Magnet-Suspension-Balance," in *Proceedings of the Annual Technical Conference of the Society of Plastics (ANTEC)*, Atlanta, USA, pp. 1918–1921, 1998.
- Pieperbeck, N., R. Kleinrahm, and W. Wagner, "Results of (Pressure, Density, Temperature) Measurements on Methane and on Nitrogen in the Temperature Range from 273.15 K to 323.15 K at Pressures up to 12 MPa Using a New Apparatus for Accurate Gas-Density Measurements," *J. Chem. Therm.*, **23**, 175–194 (1991).
- Reid, R.C., B.E. Poling, and J.M. Prausnitz, *The Properties of Gases and Liquids*, McGraw-Hill Book, New York, 1989.
- Robens, E., J.U. Keller, C.H. Massen, and R. Staudt, "Sources of Error in Sorption and Density Measurements," *Journal of Thermal Analysis and Calorimetry*, **55**, 383–387 (1999).
- Rouquerol, F., J. Rouquerol, and K. Sing, *Adsorption by Powders and Solids*, Academic Press, London, 1999.
- Sing, K.S.W. et al., "Reporting Physisorption Data for Gas/Solid Systems with Special Reference to the Determination of Surface Area and Porosity," *Pure & Appl. Chem.*, **57**, 603–619 (1985).
- Sircar, S., "Excess Properties and Thermodynamics of Multicomponent Gas Adsorption," *J. Chem. Soc. Faraday Trans 1*, **81**, 1541 (1985).
- Sircar, S., "Measurement of Gibbsian Surface Excess," *AIChE Journal*, **47**, 1169–1176 (2001).
- Staudt, R., S. Bohn, F. Dreisbach, and J.U. Keller, "Gravimetric and Volumetric Measurements of Helium Adsorption Equilibria on Different Porous Solids," in *Characterization of Porous Solids 4*, B. McEnaney et al. (Eds.), pp. 261–266, Royal Society of Chemistry, London, 1997.
- Staudt, R., G. Saller, M. Tomalla, and J.U. Keller, "A Note on Gravimetric Measurements of Gas-Adsorption Equilibria," *Ber. Bunsenges. Phys. Chem.*, **97**, 98–105 (1993).
- Stolle, R. and G. Wahl, "Deposition of Boron Nitride Films from BB'B"-Trichloroborazine," *Journal de Physique IV*, **5**, 761–768 (1995).
- Toth, J., "Isotherm Equations for Monolayer Adsorption of Gases on Heterogeneous Solid Surfaces," in *Proceedings of the 1st Intl. Conference on Fundamentals of Adsorption*, Germany, A.L. Myers and G. Belfort (Eds.), 1984.
- Wagner, W., K. Brachthäuser, R. Kleinrahm, and H.W. Lösch, "A New, Accurate Single-Sinker Densitometer for Temperatures from 233 to 523 K at Pressures up to 30 MPa," *Intl. Journal of Thermophysics*, **16**, 399–411 (1995).
- Young, D.M. and A.D. Crowell, *Physical Adsorption of Gases*, Butterworth, London, 1962.